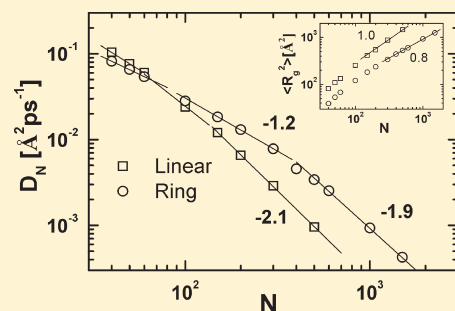


Chain Dynamics of Ring and Linear Polyethylene Melts from Molecular Dynamics Simulations

Kahyun Hur,[†] Cheol Jeong,[†] Roland G. Winkler,^{*,‡} Naida Lacevic,[§] Richard H. Gee,[§] and Do Y. Yoon^{*,†}[†]Department of Chemistry, Seoul National University, Seoul, 151-747, Korea[‡]Institut für Festkörperforschung, Forschungszentrum Jülich, D-52425 Jülich, Germany[§]Chemical Sciences Division, Lawrence Livermore National Laboratory, Livermore, California 94550, United States

ABSTRACT: The dynamical characteristics of ring and linear polyethylene (PE) molecules in the melt have been studied by employing atomistic molecular dynamics simulations for linear PEs with carbon atom numbers N up to 500 and rings with N up to 1500. The single-chain dynamic structure factors $S(q,t)$ from entangled linear PE melt chains, which show strong deviations from the Rouse predictions, exhibit quantitative agreement with experimental results. Ring PE melt chains also show a transition from the Rouse-type to entangled dynamics, as indicated by the characteristics of $S(q,t)$ and mean-square monomer displacements $g_1(t)$. For entangled ring PE melts, we observe $g_1(t) \sim t^{0.35}$ and the chain-length dependence of diffusion coefficients $D_N \propto N^{-1.9}$, very similar to entangled linear chains. Moreover, the diffusion coefficients D_N remain larger for the entangled rings than the corresponding entangled linear chains, due to about a 3-fold larger chain length for entanglement. Since rings do not reptate, our results point toward other important dynamical modes, based on mutual relaxations of neighboring chains, for entangled polymers in general.



INTRODUCTION

The conformational and dynamical properties of polymer chains in the melt strongly depend upon various molecular parameters such as molecular weight and chain architecture. For polymers of sufficiently high molecular weight, topological restrictions, which are caused by the noncrossability constraint of neighboring chains and are commonly denoted as entanglements, induce a pronounced change in the chain dynamics. The dynamical characteristics of such entangled polymer melts may be idealized by the reptation model^{1,2} and its subsequent improvements, which include additional features such as contour-length fluctuations of chains and constraint release of the confining tube.³ The theoretical models have been tested extensively by experiment^{4–7} and computer simulations,^{8–15} with reasonably successful outcome. In the reptation-based models, the chain ends play a most dominant role in determining the relaxation dynamics. It then follows that ring polymers, which obviously have no chain ends, should exhibit distinctly different chain dynamics. Up to now, there is no plausible theoretical model that describes the dynamics of ring polymers in entangled melts. An idealized model for a single ring polymer in an array of obstacles (like in a cross-linked network), denoted as “lattice animal”, predicts the center-of-mass diffusion coefficient D dependence on the molecular weight M as $D \propto M^{-2}$.^{16,17} However, the applicability of this single chain model to ring melts is subject to serious questions since it does not correctly include topological interactions and mutual relaxation effects⁵ of the neighboring ring chains. For example, it does not correctly describe the equilibrium chain conformations in ring melts (see below).

Extensive experimental studies of the chain conformations,^{18,19} diffusion coefficients,^{20–22} and rheological properties^{23–26} of various ring polymer systems in the melt have been carried out for more than 20 years. However, the experimental results are still unsettled, since the preparation of unknotted and nonconcatenated pure ring polymers of high molecular weights is an unresolved issue so far. Monte Carlo (MC) simulation studies based on the bond fluctuation model (BFM)^{27–31} and the lattice model employing nonlocal moves^{32,33} provide a valuable insight into the general conformational and dynamical characteristics. However, the detailed chain dynamics over a broad range of time scales, which is strongly affected by the nature of collapsed conformations in ring polymer melts,³⁴ is not easily accessible by coarse MC simulations. Molecular dynamics simulations of low-molecular PE ring melts have been performed in refs 34 and 35 using a united-atom model. However, further experimental, simulation, and theoretical studies are needed to gain deeper insight into the dynamics of large-ring polymer melts. Moreover, careful studies of ring polymers, with no chain ends, will provide very important insight concerning the relative importance of chain-end effects on dynamical characteristics of macromolecules in a broad range of scientific topics ranging from polymer physics³⁶ to gene expression of chromosomes in biological systems.^{22,37,38}

In this article, we present large-scale atomistic molecular dynamics simulation results of linear and ring polyethylene

Received: November 22, 2010

Revised: February 7, 2011

Published: March 04, 2011

Table 1. Simulation Parameters and Results^a

N	M	linear			ring		
		d [Å]	$\langle R_g^2 \rangle$ [Å ²]	D_N [Å ² ps ⁻¹]	d [Å]	$\langle R_g^2 \rangle$ [Å ²]	D_N [Å ² ps ⁻¹]
40	30	33.90	81.18	0.104	33.25	39.19	0.082
50	30	36.34	108.6	0.076	35.77	53.29	0.064
60	30	38.51	133.6	0.060	38.00	67.57	0.054
100	30	45.35	254.7	0.024	45.01	120.6	0.028
150	40	56.96	407.6	0.012	56.69	181.2	0.018
200	40	62.57	546.6	0.0066	62.37	237.6	0.013
300	70	85.97	851.5	0.0029	85.85	338.0	0.0078
400	70				94.50	442.8	0.0046
500	125	123.77	1450	0.000956	123.5	526.5	0.0034
600	125				131.3	597.6	0.00253
1000	125				155.7	925.9	0.000933
1500	125				178.2	1244	0.000425

^a N = number of carbon atoms; M = number of chains in the melts; d = size of simulation box.

(PE) molecules in the melt employing a well-confirmed atomistic force field.^{34,39} The largest PE ring we studied, with the total carbon number $N = 1500$, is commensurate with the recent experimental study on polystyrene rings,²⁰ as normalized by the critical entanglement length (see below). Therefore, our studies provide detailed quantitative insight into the dynamics of pure unknotted, nonconcatenated ring polymers in melts covering the crossover region from the Rouse to entangled dynamics and can serve as benchmark for future experimental and theoretical studies.

MODEL

The methylene and methyl groups of a polymer molecule are described within a united atom model, which interact with each other by a Lennard-Jones potential.^{34,39} The force field, which includes bending and torsional contributions, is described in detail in ref 39. The simulation temperature and pressure are 509 K and 1 atm, respectively. The simulated polymer lengths and system characteristics are listed in Table 1. We like to emphasize that the linear dimension of the periodic cubic simulation box is 4–5 times larger than the average radius of gyration of the polymers for all the simulated chain lengths.

Simulations of linear and ring PE chains up to $N = 300$ were reported previously.³⁴ Simulations of larger polymer systems have been performed at the Lawrence Livermore National Laboratory employing the LAMMPS code,⁴⁰ upon carefully comparing and checking the previous results of linear and ring melts for $N = 300$.³⁴ The equilibrated states of polymer melts were checked by ascertaining that two distinctly different initial configurations of highly extended chains and collapsed coiled chains led to the identical structural characteristics such as radius of gyration, monomer pair correlation function, and trans conformer population. Earlier simulations of an unentangled linear PE melt with $N = 100$ provided quantitative agreement of the dynamic structure factor $S(q,t)$ between simulations and experiments.³⁶ Here, we first demonstrate that our atomistic simulation method provides quantitative agreement with experiments for the dynamic structure factor $S(q,t)$ of an entangled linear PE melt as well. Hence, our simulation results are expected to provide a quite accurate, quantitative comparison of the

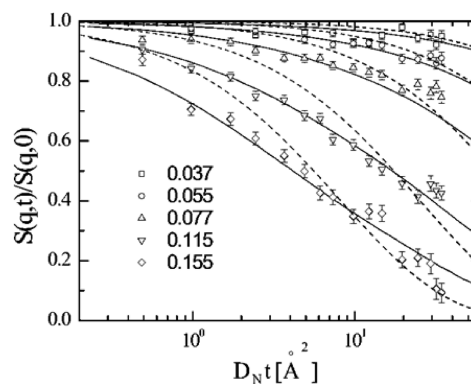


Figure 1. Single-chain dynamic structure factors $S(q,t)$ of linear PE chains in a melt. The time axis is scaled by the respective center-of-mass diffusion coefficient. The scattering vectors q are 0.037, 0.055, 0.077, 0.115, and 0.155 Å⁻¹ (top to bottom). Symbols indicate neutron scattering experimental results⁶ of linear PE with $N \approx 340$ at 509 K, solid lines the simulations results for linear PE with $N = 300$, and dotted lines the Rouse predictions for linear PE with $N = 300$.

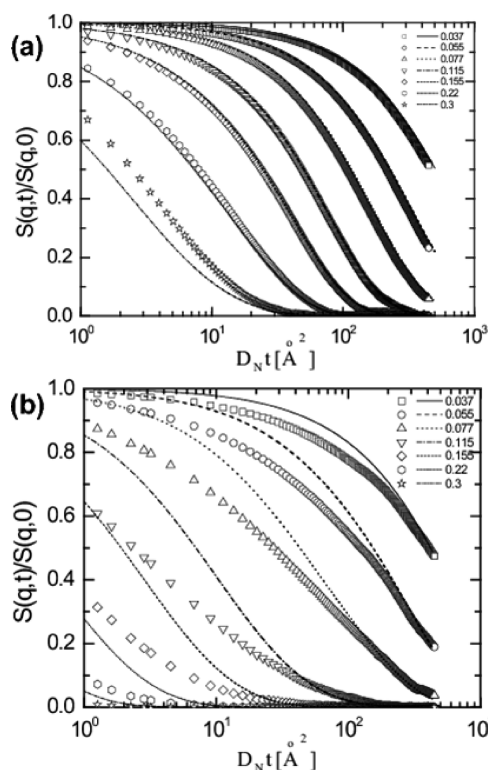


Figure 2. $S(q,t)$ of ring PE molecules in a melt with $N = 100$ (a) and 1500 (b). The time axis is scaled by the respective center-of-mass diffusion coefficient. The scattering vectors q are 0.037, 0.055, 0.077, 0.115, 0.155, 0.22, and 0.3 Å⁻¹ (top to bottom). Symbols correspond to simulation data and solid lines are predictions by the Rouse model.

dynamical characteristics of linear and pure ring polymers in entangled melts.

RESULTS

The single-chain dynamic structure factor $S(q,t)$ of linear PE molecules with $N = 300$, which is well above the critical entanglement length $N_e \approx 140$ obtained by experiment,⁶ is displayed in Figure 1 for various scattering vectors. The simulation data are in

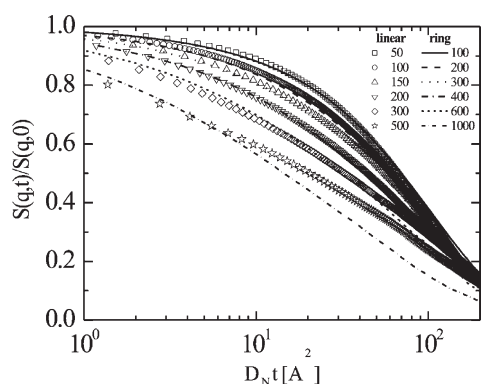


Figure 3. $S(q,t)$ of ring and linear PE molecules in a melt for $q = 0.1 \text{ \AA}^{-1}$. The time axis is scaled by the respective center-of-mass diffusion coefficient. Symbols correspond to linear chains and lines are for rings. The carbon atom numbers of the linear chains are $N = 50, 100, 150, 200, 300$, and 500 and those of rings are $N = 100, 200, 300, 600$, and 1000 (top to bottom); i.e., they are paired by a factor of 2.

quantitative agreement with the results of $S(q,t)$ obtained from neutron scattering experiments for $N \approx 340$,⁶ even though there is a slight difference in N by 40. Hence, our simulation method captures the fundamental interactions in both unentangled³⁶ and entangled PE melts, and thus is capable of providing a quantitative description of real polymer dynamics. As expected, the theoretical curves predicted by the Rouse model,² which assumes unhindered isotropic motion of a chain, disagree with the experiment and simulation results at all scattering vectors, as clearly seen in Figure 1.

The dynamic structure factor for unentangled linear polymer melts up to approximately $N \approx 100$ can be reasonably well described by the Rouse model² within a certain range of scattering vectors which depends on N (for $N = 100$, $q \leq 0.18 \text{ \AA}^{-1}$).^{36,41} Similarly, the Rouse model for ring polymers describes $S(q,t)$ for small N very well. Figure 2a exhibits good agreement between simulations and the Rouse predictions for rings with $N = 100$ up to $q = 0.22 \text{ \AA}^{-1}$. Hence, the large-scale dynamics of small rings is well described by the Rouse dynamics. Monomer correlations on smaller scales lead to deviations from the Rouse model at high scattering vectors, which can partially be captured by a persistent length in a manner similar to that for linear molecules.⁴¹ However, below a certain length scale the detailed local polymer structure determines its dynamical behavior, which cannot be captured by a coarse-grained model. Contrary to ring PE melts with $N = 100$, $S(q,t)$ for $N = 1000$ (Figure 2b) strongly deviates from the Rouse predictions even at the smallest q value 0.037 \AA^{-1} . (Note that for $q^2 \langle R_g^2 \rangle \ll 1$, where $\langle R_g^2 \rangle$ is the mean square radius of gyration, the dynamic structure factor decays as $S(q,t) \sim \exp(-q^2 D_N t)$, with D_N the diffusion coefficient for the molecule with N skeletal carbons.) At large times, the $S(q,t)$ curves of the simulations merge to the time dependence predicted by the Rouse model for all considered q vectors, as expected.² However, the decay rates at intermediate times are smaller than predicted by the Rouse model and reflect entanglement effects.

As shown in Figure 3, the dynamics of short linear PE molecules and ring PEs of twice the chain length exhibit striking similarities on larger length scales $q = 0.1 \text{ \AA}^{-1}$. Note that the mean square radius of gyration of a linear Gaussian polymer is twice as large as that of a ring molecule with the same number of monomers. This coincidence breaks down for large ring PEs with $N \geq 500$ and linear PEs with $N \geq 300$, and the ring polymers

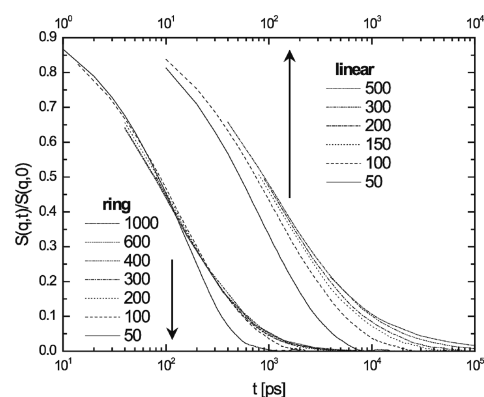


Figure 4. $S(q,t)$ of ring (left set of curves, bottom x scale) and linear (right set of curves, top x scale) PE molecules in a melt for $q = 0.3 \text{ \AA}^{-1}$. The carbon atom numbers of the rings are $N = 50, 100, 200, 300, 400, 600$, and 1000 and those of linear chains $N = 50, 100, 150, 200, 300$, and 500 (bottom to top).

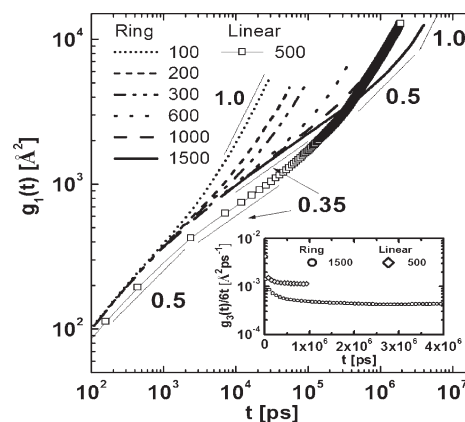


Figure 5. Mean-square displacements of monomers $g_1(t)$ for ring (lines) and linear (squares) PE molecules in a melt. The limiting slopes are indicated as number and thin lines. Inset: Scaled center-of-mass mean-square displacements $g_3(t)$ for ring (circles) and linear (diamonds) PE molecules.

exhibit a faster relaxation on large time scales. We attribute the different dynamical behavior to the collapsed chain conformations and hence weaker entanglements of rings in the melt.³⁴ Detailed analyses of the simulation data for large q values (i.e., short length scales) exhibit interesting differences in the dynamics of linear and ring PE molecules. As shown in Figure 4, the dynamics of linear PE chains depends significantly on chain length for $q = 0.3 \text{ \AA}^{-1}$. This is in contrast to the behavior of ring PE molecules, where for $N \geq 100$, we find almost identical dynamical structure factors up to large times. Only $S(q,t)$ for $N = 50$ deviates from the general behavior. The reason seems to be that small rings with $N < 100$ do not exhibit the same melt density as the larger rings, and this density effect is reflected in the monomer displacement behavior at short times.³⁴ In comparison, the melt density of linear PE chains shows a more pronounced chain-length dependence due to chain-end effects and the monomer displacements at short times reflects this chain-length effect on melt density.³⁴ Therefore, the dynamic structure factor $S(q,t)$ at larger q vectors directly reflects the monomer displacements at short times, i.e., monomer friction coefficients, which in turn depend on the melt density.

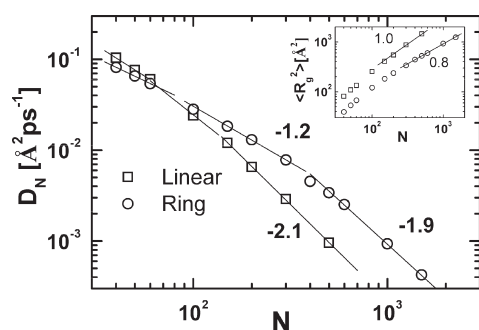


Figure 6. Diffusion coefficients D_N for ring and linear PE molecules in a melt as a function of chain length (the total carbon atom number N). The inset displays the dependence of the mean-square radii of gyration on N for melt PEs. Circles correspond to rings and squares to linear molecules. The limiting slopes are indicated as numbers and lines.

Further insight into the dynamics of ring PE melts can be obtained by the monomer mean square displacement $g_1(t)$ as depicted in Figure 5. For small ring melts up to $N = 100$, $g_1(t)$ shows a crossover from a $t^{0.5}$ power-law Rouse regime to the free diffusion regime $t^{1.0}$. With increasing chain length, an intermediate time regime develops, with a slope significantly smaller than $1/2$. For the ring system with $N = 1500$, we find the dependence $t^{0.35}$. This slowdown reflects the presence of entanglements. On larger time scales, the mean square displacement crosses over to a linear dependence corresponding to free diffusion. In comparison, the entangled linear PE melt with $N = 500$, displayed in Figure 5, also exhibits an intermediate time regime with the dependence $t^{0.35}$. A similar dynamical slowdown, $g_1(t) \sim t^{0.4}$, was observed previously for entangled melts of linear PE¹² and poly(butadiene).¹³ Here, it is evident that the asymptotic limit $g_1(t) \sim t^{0.25}$ predicted for a linear chain in reptation¹ is not observed yet.

The dependence of the self-diffusion coefficient D_N on the chain length is presented in Figure 6. D_N is obtained from the long-time plateau value of $g_3(t)/6t$, where $g_3(t)$ is the chain center-of-mass mean-square displacement, as illustrated in the inset of Figure 5 for the largest linear ($N = 500$) and ring ($N = 1500$) PEs simulated in this work. For linear PEs we observe a crossover from the dependence $D_N \propto N^{-1.4}$ to $D_N \propto N^{-2.1}$ (for the largest 3 chains), which is attributed to the presence of entanglements.¹ The exponent -2.1 was also seen in previous simulations of poly(butadiene) melts¹³ and is in close agreement with the value -2.3 from experiments,⁴ Monte Carlo and molecular dynamics simulations,^{9,35} within limits of simulations. For larger ring PEs, we find the chain-length dependence $D_N \propto N^{-1.9}$ (for the largest three chains); i.e., the exponent for rings is only slightly smaller in magnitude than that for linear PEs in entangled melts. Moreover, the ring diffusion coefficients exhibit a broad crossover regime from unentangled to entangled dynamics, which we attribute to the chain collapse,^{18,19,28,34,35,42} as shown by the inset of Figure 6. Previously, a BFM simulation²⁸ reported the dependence $D_N \propto N^{-1.59}$, whereas a range of exponents from -1.2 to -1.7 was seen by Monte Carlo simulations depending on the chain flexibility.³⁰ Considering that these simulations were performed at a lower polymer concentration than typical polymer melt values, our result $D_N \propto N^{-1.9}$ together with $g_1(t) \sim t^{0.35}$ for fully atomistic simulations represents a more accurate description of entangled ring polymer melts. However, the origin of the dependence $D_N \propto N^{-1.9}$ should be different from the lattice animal prediction,¹⁷ where the exponent

of the radius of gyration is proposed to be $\nu = 0.25$, but the rings studied in our simulations exhibit $\nu = 0.4$ (for the largest 5 chains), as shown in the inset of Figure 6.

The critical entanglement length of linear PE obtained experimentally by Richter et al.⁶ is $N_e \approx 140$, consistent with our simulation results (Figure 6), whereas the corresponding value of ring PE seems to be approximately $N_e \approx 400$, which is the critical chain length at which the diffusion-coefficient exponent changes slope from -1.2 to -1.9 . Interestingly, the estimated value of the mean-square radius of gyration at critical entanglement length N_e is $\langle R_g^2 \rangle \approx 440 \text{ Å}^2$, for both the linear and the ring PE melt, which might suggest that the entanglement constraint on the lateral motion sets in at a similar length scale.

CONCLUSIONS

We have observed a good quantitative agreement between dynamic structure factors $S(q,t)$ from simulation data and neutron scattering experiments on linear PE melts with $N \approx 300$, which exhibit strong deviation from the Rouse-model predictions due to entanglements. The dynamics of large rings in the melt is influenced by both chain collapse and entanglements, leading to a broad crossover regime from unentangled to entangled dynamics with the critical chain length for entanglements about three times larger than that for linear chains. The chain-length dependence of the diffusion coefficients $D_N \propto N^{-1.9}$ and the observed $g_1(t) \sim t^{0.35}$ behavior of ring chains in entangled melts are both very similar to the characteristics of linear chains. Moreover, the diffusion coefficients D_N remain larger for the entangled rings than the corresponding entangled linear chains, as has also been found experimentally for DNA rings in entangled solutions.²² This may arise from the larger critical chain length for entanglements of rings than the linear chains at the same volume fraction. Since rings do not reptate, our results point toward other important dynamical modes, based on mutual relaxations of neighboring chains, for entangled polymers in general. Further studies on linear and ring polymers of far greater chain lengths are now critically needed to ascertain this finding and to understand the dynamics of highly entangled polymers in the asymptotic region.⁴³

AUTHOR INFORMATION

Corresponding Author

*E-mail: D.Y.Y., dyoon@snu.ac.kr; R.G.W., r.winkler@fz-juelich.de.

ACKNOWLEDGMENT

We thank D. Richter and K. Kremer for helpful discussions and acknowledge the financial support by the National Research Foundation of Korea (R01-2008-000-11971-0), Korea Institute of Science and Technology Information (KSC-2009-S03-0006), and the Chemistry and Molecular Engineering Program of Brain Korea 21 Project. Portions of this work were performed under the auspices of the U.S. Department of Energy by Lawrence Livermore National Laboratory under Contract DE-AC52-07NA27344.

REFERENCES

- (1) de Gennes, P. G. *J. Chem. Phys.* **1971**, *55*, 572–575.
- (2) Doi, M.; Edwards, S. F. In *The Theory of Polymer Dynamics*; Oxford University: Oxford, U.K., 1986.
- (3) McLeish, T. C. B. *Adv. Phys.* **2002**, *51*, 1379–1527.
- (4) Lodge, T. P. *Phys. Rev. Lett.* **1999**, *83*, 3218–3221.

- (5) Liu, C. Y.; Keunings, R.; Bailly, C. *Phys. Rev. Lett.* **2006**, 97, 246001.
- (6) Richter, D.; Willner, L.; Zirkel, A.; Farago, B.; Fetters, L. J.; Huang, J. S. *Macromolecules* **1994**, 27, 7437–7446.
- (7) Wischniewski, A.; Monkenbusch, M.; Willner, L.; Richter, D.; Likhtman, A. E.; McLeish, T. C. B.; Farago, B. *Phys. Rev. Lett.* **2002**, 88, 058301.
- (8) Kremer, K.; Grest, G. S. *J. Chem. Phys.* **1990**, 92, 5057–5086.
- (9) Hagita, K.; Takano, H. *J. Phys. Soc. Jpn.* **2003**, 72, 1824–1827.
- (10) Everaers, R.; Sukumaran, S. K.; Grest, G. S.; Svaneborg, C.; Sivasubramanian, A.; Kremer, K. *Science* **2004**, 303, 823–826.
- (11) Padding, J. T.; Briels, W. J. *J. Chem. Phys.* **2002**, 117, 925–943.
- (12) Harmandaris, V. A.; Mavrantzas, V. G.; Theodorou, D. N.; Kroger, M.; Ramirez, J.; Ottinger, H. C.; Vlassopoulos, D. *Macromolecules* **2003**, 36, 1376–1387.
- (13) Tsolou, G.; Mavrantzas, V. G.; Theodorou, D. N. *Macromolecules* **2005**, 38, 1478–1492.
- (14) Kröger, M. *Phys. Rep.* **2004**, 390, 453–551.
- (15) Stephanou, P. S.; Baig, C.; Tsolou, G.; Mavrantzas, V. G.; Kröger, M. *J. Chem. Phys.* **2010**, 132, 124904.
- (16) Rubinstein, M. *Phys. Rev. Lett.* **1986**, 57, 3023–3026.
- (17) Obukhov, S. P.; Rubinstein, M.; Duke, T. *Phys. Rev. Lett.* **1994**, 73, 1263–1266.
- (18) Arrighi, V.; Gagliardi, S.; Dagger, A. C.; Semlyen, J. A.; Higgins, J. S.; Shenton, M. J. *Macromolecules* **2004**, 37, 8057–8065. Gagliardi, S.; Arrighi, V.; Ferguson, R.; Dagger, A. C.; Semlyen, J. A.; Higgins, J. S. *J. Chem. Phys.* **2005**, 122, 064904.
- (19) Ohta, Y.; Masuoka, K.; Takano, A.; Matsushita, Y. *Physica B* **2006**, 385, 532–534.
- (20) Kawaguchi, D.; Masuoka, K.; Takano, A.; Tanaka, K.; Nagamura, T.; Torikai, N.; Dalglish, R. M.; Langridge, S.; Matsushita, Y. *Macromolecules* **2006**, 39, 5180–5182.
- (21) von Meerwall, E.; Ozisik, R.; Mattice, W. L.; Pfister, P. M. *J. Chem. Phys.* **2003**, 118, 3867–3873.
- (22) Robertson, R. M.; Smith, D. E. *Proc. Natl. Acad. Sci. U. S. A.* **2007**, 104, 4824–4827.
- (23) McKenna, G. B.; Hadziioannou, G.; Lutz, P.; Hild, G.; Strazielle, C.; Straupe, C.; Rempp, P.; Kovacs, A. J. *Macromolecules* **1987**, 20, 498–512.
- (24) McKenna, G. B.; Hostetter, B. J.; Hadjichristidis, N.; Fetters, L. J.; Plazek, D. J. *Macromolecules* **1989**, 22, 1834–1852.
- (25) Roovers, J. *Macromolecules* **1988**, 21, 1517–1521.
- (26) Kapnistos, M.; Lang, M.; Vlassopoulos, D.; Pyckhout-Hintzen, W.; Richter, D.; Cho, D.; Chang, T.; Rubinstein, M. *Nat. Mater.* **2008**, 7, 997–1002.
- (27) Brown, S.; Szamel, G. *J. Chem. Phys.* **1998**, 109, 6184–6192.
- (28) Brown, S.; Lenczycki, T.; Szamel, G. *Phys. Rev. E* **2001**, 63, 052801.
- (29) Müller, M.; Wittmer, J. P.; Cates, M. E. *Phys. Rev. E* **1996**, 53, 5063–5074.
- (30) Müller, M.; Wittmer, J. P.; Cates, M. E. *Phys. Rev. E* **2000**, 61, 4078–4089.
- (31) Suzuki, J.; Takano, A.; Deguchi, T.; Matsushita, Y. *J. Chem. Phys.* **2009**, 131, 144902.
- (32) Vettorel, T.; Reigh, S. Y.; Yoon, D. Y.; Kremer, K. *Macromol. Rapid Commun.* **2009**, 30, 345–351.
- (33) Vettorel, T.; Grosberg, A. Y.; Kremer, K. *Phys. Biol.* **2009**, 6, 025013.
- (34) Hur, K.; Winkler, R. G.; Yoon, D. Y. *Macromolecules* **2006**, 39, 3975–3977.
- (35) Tsolou, G.; Stratikis, N.; Baig, C.; Stephanou, P. S.; Mavrantzas, V. G. *Macromolecules* **2010**, 43, 10692–10713.
- (36) Paul, W.; Smith, G. D.; Yoon, D. Y.; Farago, B.; Rathgeber, S.; Zirkel, A.; Willner, L.; Richter, D. *Phys. Rev. Lett.* **1998**, 80, 2346–2349.
- (37) Lancot, C.; Cheutin, T.; Cremer, M.; Cavalli, G.; Cremer, T. *Nat. Rev. Genet.* **2007**, 8, 104–115.
- (38) Rosa, A.; Everaers, R. *PLoS Comput. Biol.* **2008**, 4, e1000153.
- (39) (a) Chang, J.; Han, J.; Yang, L.; Jaffe, R. L.; Yoon, D. Y. *J. Chem. Phys.* **2001**, 115, 2831–2840. (b) Paul, W.; Yoon, D. Y.; Smith, G. D. *J. Chem. Phys.* **1995**, 103, 1702–1709.
- (40) Plimpton, S. J. *Comput. Phys.* **1995**, 117, 1–19.
- (41) Harnau, L.; Winkler, R. G.; Reineker, P. *Europhys. Lett.* **1999**, 45, 488–494.
- (42) Müller, M.; Wittmer, J. P.; Barrat, J. L. *Europhys. Lett.* **2000**, 52, 406–412.
- (43) Rubinstein, M. *P.G. de Gennes' Impact on Science*; World Scientific Publishing Co.: Singapore, 2009; Vol. II, pp 20–58.